JOURNAL OF MATERIALS SCIENCE 29 (1994) 2095–2101

Trivalent Ce_2O_3 and CeO_{2-x} intermediate oxides induced by laser irradiation of CeO_2 powders

F. VASILIU
Research Institute for Aircraft Materials, P.O. Box 24, R-76900, Bucharest-Magurele, Romania
V. PÂRVULESCU
Institute for Non-Ferrous and Rare Metals, Bd. Biruintei 102, Bucharest, Romania
C. SÂRBU
Institute of Physics and Technology of Materials, P.O. Box MG-7, R-76900, Bucharest-Magurele, Romania

A strong non-stoichiometry of pure f c c CeO_2 was induced by laser irradiation. The increase of laser power and/or energy density had a saturable effect on particle size growth. The possibility of CeO_2 reduction to A-Ce_2O_3 by laser irradiation was demonstrated. Particles of stable Ce_7O_{12} phase were observed in all specimens irradiated at low laser-power densities. An epitaxial relationship between triclinic $Ce_{11}O_{20}$ and cubic $Ce_{12}O_{22}$ phases was found. The controversial C-Ce_2O_3 phase was detected at the limits of a b c c particle. An unknown b c c phase of acicular morphology, strongly related to C-Ce_2O_3, was also registered. The dose dependence of CeO_2 structural modifications obtained by laser irradiation as a function of laser energy density variation could be explained by a simple defect aggregation model implying lattice defects (oxygen vacancies and Ce^{3+} ions).

1. Introduction

It is now well established that bulk cerium oxides are classified according to the oxidation state of the rare-earth element as: divalent, CeO (obtained under high pressures and temperatures); trivalent, Ce_2O_3; and tetravalent and intermediate oxides, CeO_2 and CeO_{2-x} [1, 2]. Two polymorphic compounds Ce_2O_3 are also reported: A-Ce_2O_3 (hexagonal, space group $P\bar{3}$ ml) and the controversial C-Ce_2O_3 (cubic, space group T_h^7 or Ia3) [1, 2]. Structure and sintaxy of R_2O_3 (R = rare-earth element) oxides and their relationship to the fluorite structure of RO_2 have been investigated in great detail [3, 4].

The intermediate oxides associated with various rare-earth elements (including cerium) can be described by the equivalent basic formulae: RO_x ($1.5 \leqslant x \leqslant 2$) and R_nO_{2n-2} ($4 \leqslant n < \infty$) where $n = 4$ leads to R_2O_3 and $n = \infty$ to RO_2 [4–8]. The homologous series R_nO_{2n-2} contains a great number of structures (especially hexagonal, monoclinic and triclinic) built on the fluorite-like lattice of RO_2 compound, which are due to various oxygen–vacancy rearrangement mechanisms [3, 4, 6].

Recent electron microscopy experiments demonstrated that the electron-beam irradiation induces unexpected crystallographic phase transitions in thin films of rare-earth oxides, very sensitive to experimental conditions (especially water vapour contamination) [9, 10]. On the other hand, it is well known that laser irradiation may induce or enhance such reactions as oxidation, nitridation, reduction, and doping of various materials [11–13]. High-pressure phases of SiO_2 [14] and a conversion of graphite into diamond [15] were obtained by pulsed laser fluxes impinging on the respective fine powders. More recently, a laser-induced calcite–aragonite transition [16] and a reduction of V_2O_5 by the appearance of V^{4+} and V^{3+} ions in the laser irradiated powders [17], were reported.

This paper describes the various phase transformations induced by laser irradiation in pure stoichiometric CeO_2 powders.

2. Experimental procedure

Pure CeO_2 powders were prepared by precipitation of cerium nitrate of 99.991% purity using ammonia (Merck purity). After precipitation, the samples were washed for the complete removal of ammonium nitrate, then filtered and dried at 110 °C for 8 h.

The irradiation of these specimens was done by a CO_2 laser operating in continuous wave at power densities between 0.40 and 1.30 $kW\,cm^{-2}$ and for irradiation times between 7 and 50 s (Table I).

The laser beam was focused to a spot of 39 mm^2 area. The pressure of the gas mixture was 24 torr (He, 13 torr; H_2, 9 torr; CO_2, 2 torr). The thickness of CeO_2 powder layers submitted to laser irradiation was 1.5 mm.

0022–2461

TABLE I Experimental laser irradiation parameters

Specimen	Laser-beam power density ($kW\,cm^{-2}$)	Irradiation time (s)	Laser energy density (dose)[a] ($kJ\,cm^{-2}$)
1	0.65	7	4.5
2	0.90	7	6.3
3	1.00	7	7.0
4	1.00	14	14.0
5	1.15	7	8.0
6	1.30	7	9.1
7	0.40	20	8.0
8	0.40	50	20.0
9	0.40	100	40.0

[a] A conventional classification of laser irradiation doses as small ($< 7\,kJ\,cm^{-2}$), mean (7–$14\,kJ\,cm^{-2}$) and high ($> 14\,kJ\,cm^{-2}$) doses, was used for easier discussion.

The CeO_2 powders were studied by conventional transmission electron microscopy (CTEM) and selected-area electron diffraction (SAED) in a TEMSCAN-100 CX (Jeol) electron microscope, operating at 200 kV, with special caution in order to eliminate any significant water-vapour contamination and temperature increase during all electronmicroscopical observations.

3. Results and discussion

The pure CeO_2 powders consist of particles having a diameter of 20–40 nm and their structure, confirmed by SAED, belongs to the cubic polycrystalline CeO_2 ($a_0 = 0.541$ nm).

In general, laser irradiation induced a variable non-stoichiometry in pure fcc CeO_2, depending on irradiation parameters. All the specimens contained, as major phase, an fcc CeO_{2-x} (where x is very small) phase, having an increased lattice parameter ($a_0 = 0.553$–0.555 nm) (Fig. 1). Particles of fcc CeO_{2-x} structure ($a_0 = 0.553$ nm) were recently obtained by a vacuum annealing technique applied to CeO_2 [18].

A saturable effect of particle-size growth, depending on the laser power and/or energy density increase, was observed (Fig. 2). For low and mean doses ($< 9\,kJ\,cm^{-2}$) only CeO_{2-x} polycrystalline diffraction rings were registered, but, for higher doses, large, thin, single-crystal CeO_{2-x} platelets occurred (Fig. 3). Sometimes, two or three single-crystal particles were joined after a prolonged irradiation (Fig. 4) due to enhanced local diffusion effects.

The possibility of CeO_2 reduction to A-Ce_2O_3 by laser irradiation at low doses was demonstrated by SAED, because single-crystal A-Ce_2O_3 particles of $\langle \bar{1}\,2\,0 \rangle$ and $\langle \bar{4}\,2\,3 \rangle$ zone axis were formed in areas also containing smaller particles of CeO_{2-x} (Fig. 5). A large single-crystal A-Ce_2O_3 platelet of the same $\langle \bar{4}\,2\,3 \rangle$ zone axis also occurred for mean doses (Fig. 6).

A mechanism currently used for non-stoichiometric oxide studies, based on the clustering of the simplest defect, consisting of an oxygen vacancy and two trivalent cations (virtually a Ce_2O_3 nucleus) resulting by laser irradiation, could explain the A-Ce_2O_3 appearance in a CeO_{2-x} lattice containing very high anion

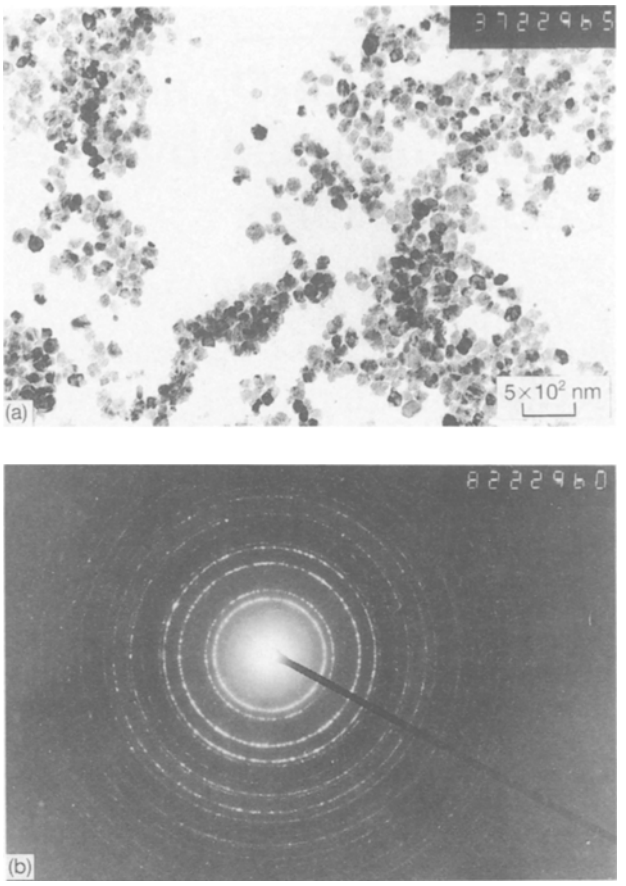

Figure 1 Small fcc CeO_{2-x} particles obtained by laser irradiation at mean doses ($9\,kJ\,cm^{-2}$): (a) TEM image, (b) SAED pattern.

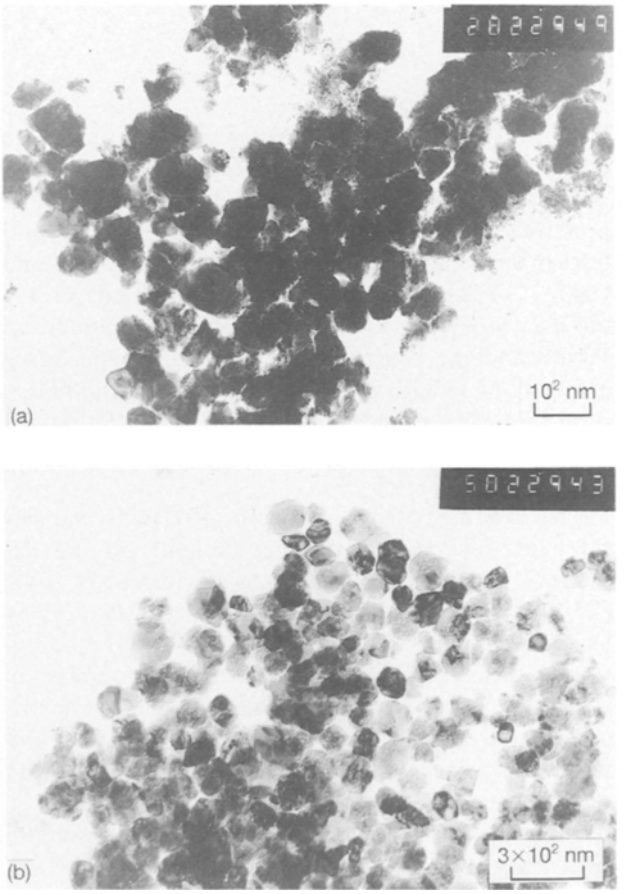

Figure 2 TEM images of CeO_{2-x} particles obtained by laser irradiation at: (a) low doses ($4.5\,kJ\,cm^{-2}$), (b) mean doses ($14\,kJ\,cm^{-2}$).

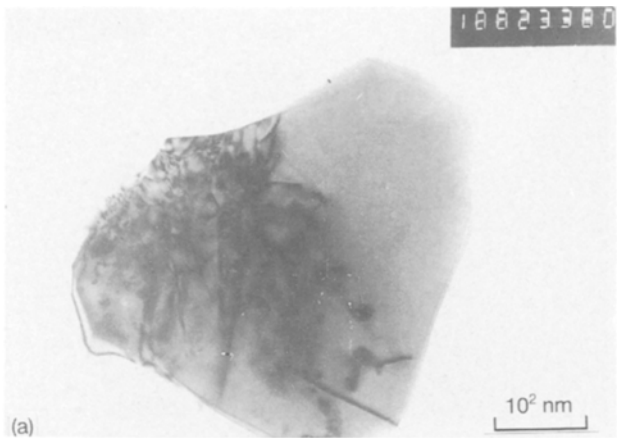

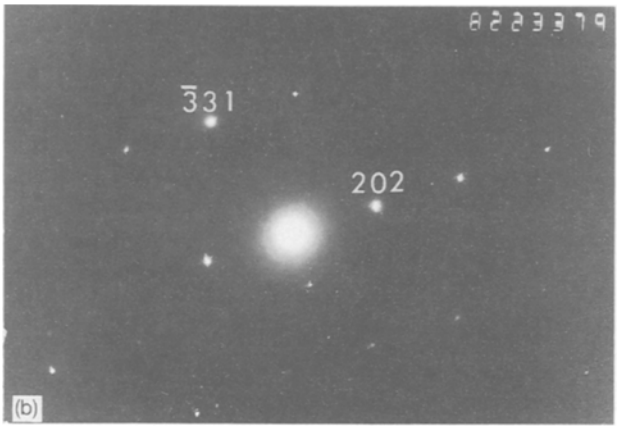

Figure 3 A very large single-crystal CeO_{2-x} particle which occurred in a specimen irradiated at high doses (40 kJ cm^{-2}): (a) TEM image, (b) $\langle 3\,4\,\bar{3} \rangle$ zone axis pattern.

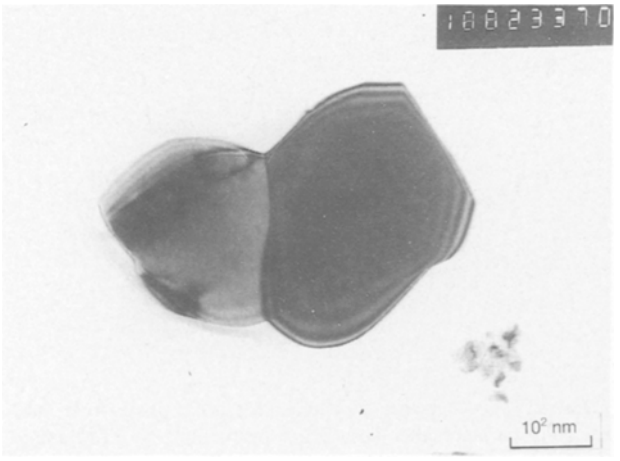

Figure 4 Joined CeO_{2-x} particles after prolonged laser irradiation (0.4 kW cm^{-2}, 50 s).

vacancy concentrations. Complete conversion of CeO_2 to A-Ce_2O_3 was not possible, at least in the range of the irradiation parameters used.

The formation of stable Ce_7O_{12} phase was detected only for low laser-power densities (0.4 kW cm^{-2}) and for mean doses ($\sim$ 8 kJ cm^{-2}) (Fig. 7) or high doses (40 kJ cm^{-2}) (Fig. 8), in the last case a particular orientation of high Miller indices being identified.

Although compounds of strange non-stoichiometry of the type formed in oxidized rare-earth thin films irradiated by energetic electron beams [9, 10, 19, 20]

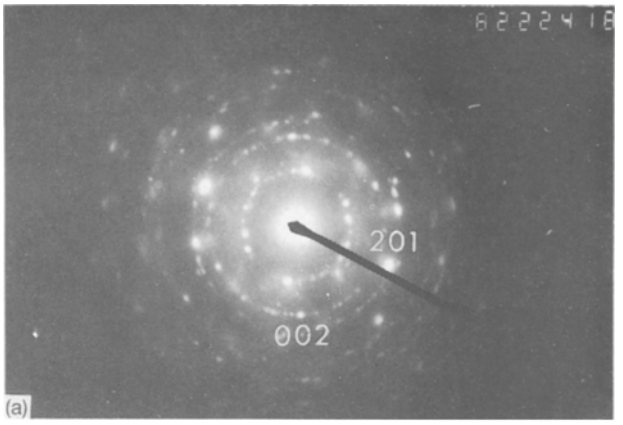

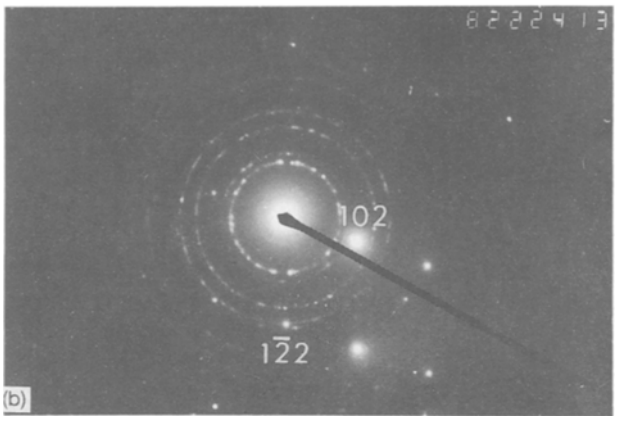

Figure 5 Single-crystal A-Ce_2O_3 particles found after laser-induced CeO_2 reduction: (a) $\langle \bar{1}\,2\,0 \rangle$ zone axis pattern, (b) $\langle \bar{4}\,2\,3 \rangle$ zone axis pattern (see also CeO_{2-x} diffraction rings).

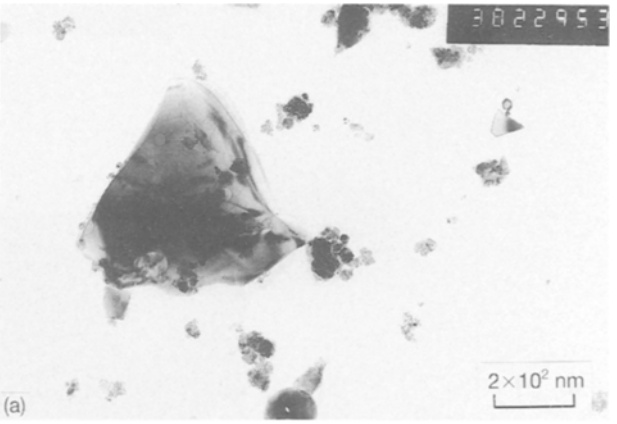

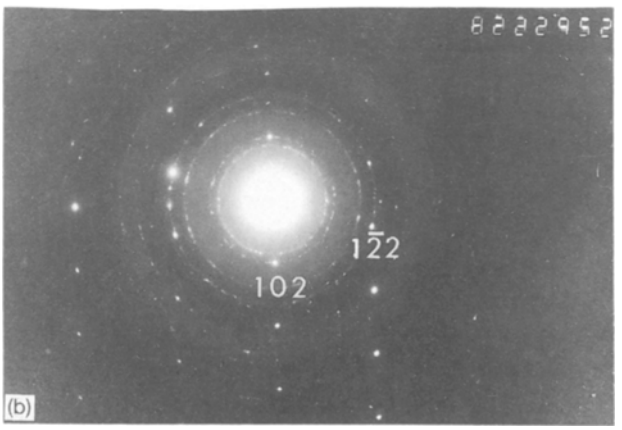

Figure 6 Large single-crystal A-Ce_2O_3 platelet appearing in laser-irradiated CeO_{2-x} at mean doses: (a) TEM image, (b) $\langle \bar{4}\,2\,3 \rangle$ zone axis pattern.

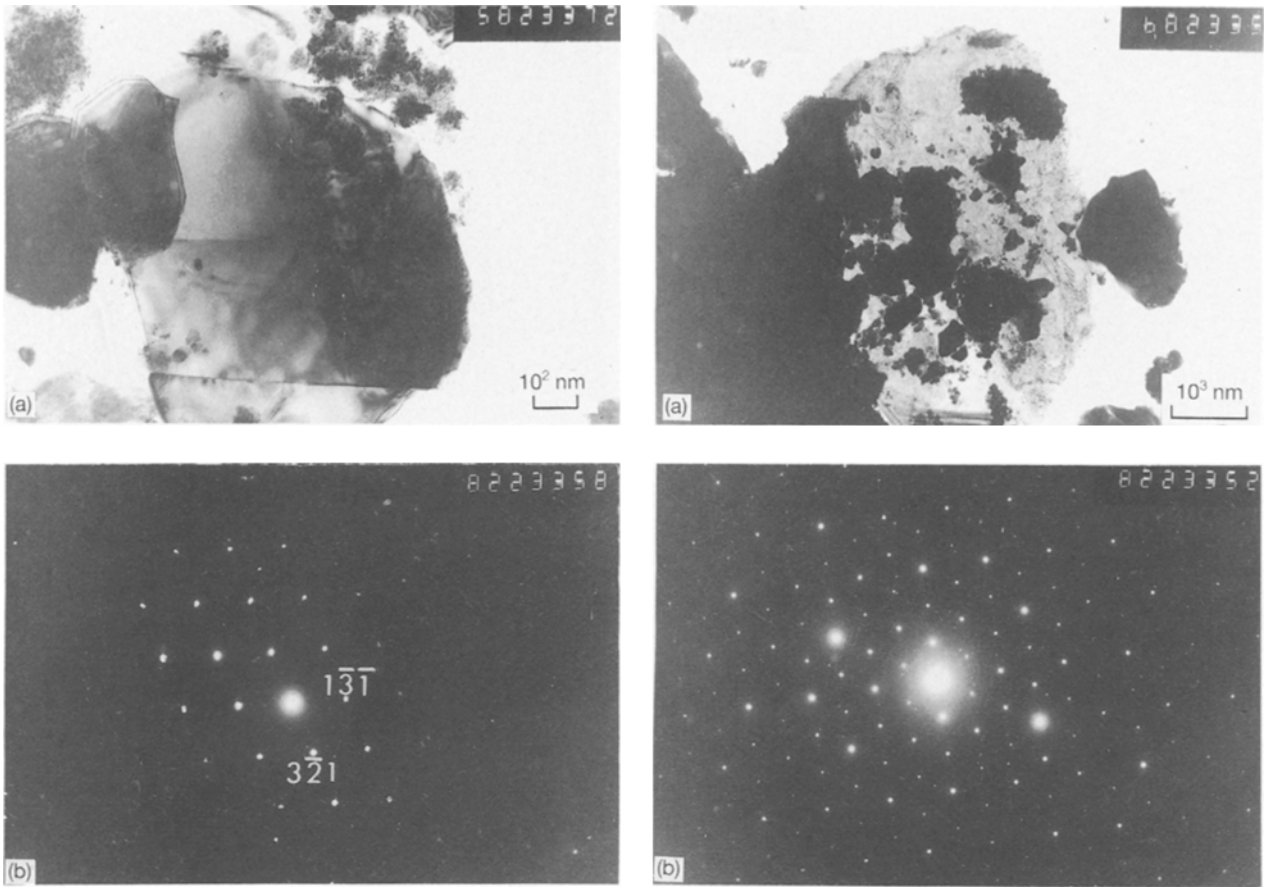

Figure 7 Particle of Ce_7O_{12} phase obtained by laser irradiation at mean doses: (a) TEM image, (b) $\langle 2\,1\,\bar{7}\rangle$ zone axis pattern.

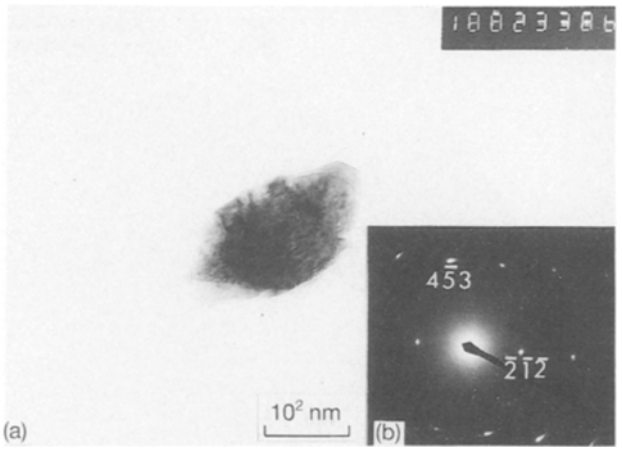

Figure 8 Another Ce_7O_{12} particle observed in a specimen irradiated at a high dose (40 kJ cm^{-2}): (a) TEM image, (b) $\langle \bar{8}\,3\,\bar{1}\,4\rangle$ zone axis pattern.

were not detected, some members of the Ce_nO_{2n-2} series of greater n values were identified in the laser-irradiated specimens for low power densities and short irradiation times. Thus, an epitaxial relationship between triclinic $Ce_{11}O_{20}$ and cubic $Ce_{12}O_{22}$ phases, after laser-beam irradiation of CeO_2 powders, was found (Fig. 9). The orientation relationships between the two phases were

$$\langle 1\,1\,0\rangle\ Ce_{11}O_{20} \parallel \langle 1\,1\,0\rangle\ Ce_{12}O_{22}$$

and

$$[1\,\bar{1}\,4]\ Ce_{11}O_{20} \parallel [\bar{1}\,1\,1]\ Ce_{12}O_{22}$$

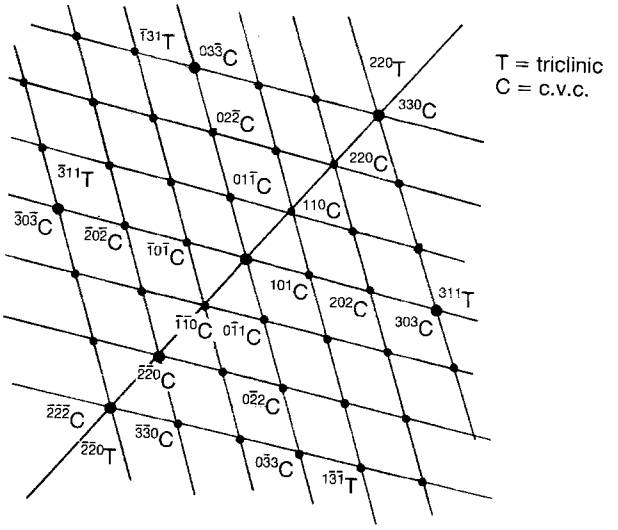

Figure 9 The occurrence of triclinic $Ce_{11}O_{20}$ phase from cubic $Ce_{12}O_{22}$ particles after laser-beam irradiation: (a) TEM image, (b) SAED pattern, (c) interpretation of SAED pattern (orientation relationships: $\langle 1\,1\,0\rangle$ $Ce_{11}O_{20} \parallel \langle 1\,1\,0\rangle$ $Ce_{12}O_{22}$ and $[1\,\bar{1}\,4]$ $Ce_{11}O_{20} \parallel [\bar{1}\,1\,1]$ $Ce_{12}O_{22}$).

The controversial C-Ce_2O_3 (Ia3) phase, having $a_c = 1.116$ nm and observed in some experiments [21, 22], was identified in our investigations as a thick quasiepitaxial layer grown at the limits of some prismatic particles with an unusual bcc structure but having a lattice parameter $a_o = 0.554$ nm (Fig. 10). By tilting of the $\langle 1\,3\,5\rangle$ zone axis SAED pattern, the new additional spots can be interpreted as belonging to C-Ce_2O_3 phase having a doubled lattice parameter ($a_C \simeq 2a_o$). A dark-field image (Fig. 10c) taken with the $(6\,3\,5)_C$ spot (Fig. 10d) confirmed the C-Ce_2O_3 phase

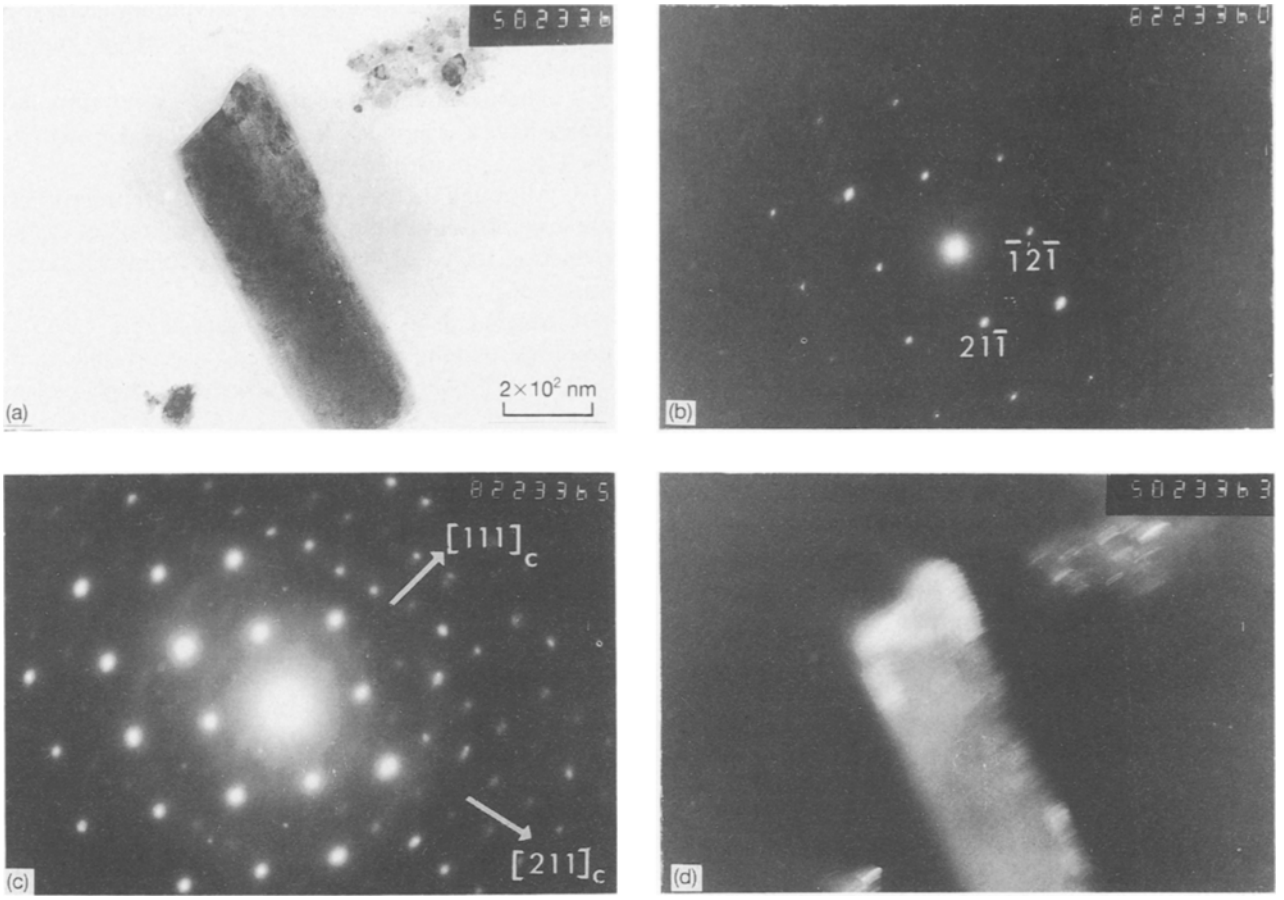

Figure 10 (a) TEM image of a prismatic particle (b c c structure: $a_o = 0.554$ nm), (b) the associated $\langle 1\,3\,5 \rangle$ zone axis pattern, (c) tilted SAED pattern with additional spots interpreted as C-Ce_2O_3 phase ($a_C \sim 2a_o$), (d) dark-field image taken with the $(6\,3\,5)_C$ spot.

occurrence. It is well known that the (1 3 5) plane is the structural feature relating the homologous series in binary rare-earth oxides [4, 6]. The odd members of the Ce_nO_{2n-2} series have $\{1\,3\,5\}$ planes that contain all the 6-coordinated rare-earth atoms with two oxygen atoms missing from each coordination cube along [1 1 1]. For even members, the defect feature is a corrugation of $\{1\,3\,5\}$ planes which result from twinning at the unit cell level. In our case, the corrugations are modified and the unit cell parameters are doubled, according to previously suggested structural principles that relate the unit cells of the members of the homologous series [5].

Another unknown b c c phase ($a_o = 1.170$ nm) of needle-like morphology (Fig. 11), strongly related to C-Ce_2O_3, was registered only in a specimen irradiated at 1 kW cm^{-2} for 7 s. The real structure of this last phase seemed to be governed by a more severe selection rule than the space group T_h^7 (Ia3) because the observed lines correspond only for $h + k + l = 4n$ (Table II), excepting the very intense (2 2 2) line of the fluorite structure. This b c c phase should be an intermediate CeO_{2-x} phase having $x \gtrsim 0.5$ and an increased lattice parameter compared to C-Ce_2O_3 phase due to a different anion vacancy arrangement at the unit cell level.

A qualitative model could explain the observed structural modifications in f c c CeO_2 subjected to laser irradiation. At small irradiation doses, the high concentration of induced oxygen vacancies will be

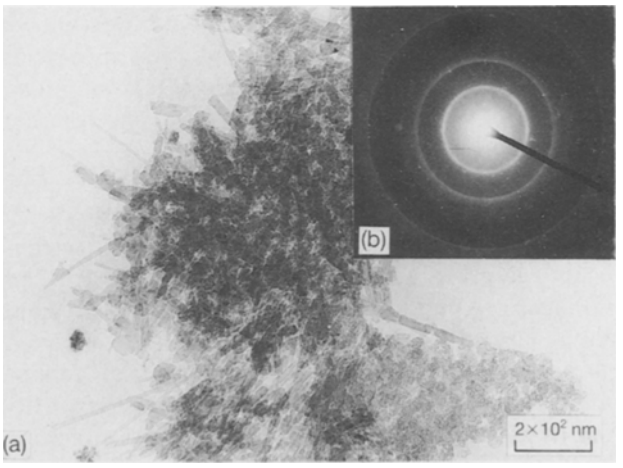

Figure 11 Needle-like particles of an unknown phase, related to C-Ce_2O_3, found after laser irradiation (7 kJ cm^{-2}): (a) TEM image, (b) SAED polycrystalline pattern.

accommodated by the open crystal structure containing multiple occupying positions for defect clusters. Because the nearest-neighbour cation sites surrounding the majority of Ce^{3+} ions will be occupied by Ce^{4+} lattice cations, the maximum extent of defect aggregation will be the formation of simple clusters involving single vacancies bound to the isolated Ce^{3+} cations. Therefore, the A-Ce_2O_3 occurrence could be explained by the clustering of one vacancy and two trivalent cations.

TABLE II Indexing of an unknown phase related to C-Ce_2O_3 phase (T_h^7 or Ia3)

2R (mm)	d_{hkl}	hkl	$I_{est.}$	$I \sim pF^2d^{2a}$	I_{calc}[b]
12.5	3.39	222	vs	100	100
20.6	2.06	044	s	66	33
25.4	1.65	444	m	19	8
35.5	1.19	804	w	37	12
41.5	1.02	088	w	13	6

[a] p, permutation factor; F, structure factor.
[b] Corrected values (taking into account the angular variation of scattering atomic factors).

At mean doses, the increased number of lattice defects (oxygen vacancies and Ce^{3+} ions) will lead to an increase of anion mobility although low mobilities should be expected in the cation sublattice. Thus, a substantial ordering of interacting defects or defect complexes will occur, resulting in the subphase Ce_nO_{2n-2} ($n > 6$) formation [23]. In the laser-irradiated CeO_2 powders, we have already detected intermediate oxide phases corresponding to $n = 7$, 11 and 12.

For high irradiation doses, it might be expected that an increasing number of clusters of two, three or more Ce^{3+} ions would be found, thus generating a random cluster distribution in the CeO_{2-x} lattice. These trivalent ions provide deeper traps for the vacancies, resulting in a reduction of oxygen vacancy mobility. The vacancy mobility decrease could be connected to the more stable phase occurrence. Large Ce_7O_{12} particles were currently observed in CeO_2 specimens subjected to laser irradiation at high doses.

Therefore, the occurrence of some well-known intermediate oxides after laser irradiation appears as due to the high sensitivity of the structural ordering to any small variation of oxygen vacancy concentration in the fluorite CeO_2 lattice.

The formation of unusual phases could be tentatively explained as a consequence of acoustic elastic waves generation by laser irradiation. The electron-beam impact has been already suggested by Gasgnier's group as being the source of high-pressure shock waves which could induce the observed paradoxical crystallography of some rare-earth intermediate oxides [9, 10, 20, 24]. Laser or electron irradiation lead to phase transition processes differing from the normal thermal annealing case, demonstrated in the case of the Jahn–Teller effect [25]. At room temperature, the induced transverse acoustic phonons result in an average displacement of the atoms from their equilibrium positions which could be approximately as large as the bond length [26]. A recent lattice dynamics calculation for high T_c superconducting oxides [27] has suggested that a coupling of acoustic waves to low-frequency oxygen modes with large amplitude of vibrations could induce phase transitions.

4. Conclusions

1. Laser irradiation induces a strong non-stoichiometry of pure stoichiometric fcc CeO_2. All the samples contain an fcc CeO_{2-x} having an increased lattice parameter ($a_o = 0.553$–0.555 nm) as major phase.

2. The laser-power density and/or energy-dose increase have a saturable effect on particle size growth in the CeO_{2-x} oxide powders.

3. Although the known CeO_2 reduction procedures are generally difficult, a new easier possibility of CeO_2 reduction to A-Ce_2O_3 by laser irradiation was demonstrated.

4. Single-crystal particles of very stable Ce_7O_{12} phase were found in all specimens laser irradiated at 0.4 kW cm^{-2} but none were detected at high power densities.

5. Although non-equilibrium compounds of strange non-stoichiometry, previously reported for rare-earth oxide thin films irradiated by electron beams, had not been observed, some unusual phases were also detected. An epitaxial relationship between triclinic $Ce_{11}O_{20}$ and cubic $Ce_{12}O_{22}$ phases was found. An unknown needle-like bcc phase and the controversial C-Ce_2O_3 phase were also registered.

References

1. M. GASGNIER, *Phys. Status Solidi (a)* **57** (1980) 11.
2. *Idem, ibid.* **114** (1989) 11.
3. G. BRAUER, in "Progress in the Science and Technology of the Rare Earths", Vol. 2 edited by L. Eyring (Pergamon Press, Oxford, 1966) p. 312.
4. L. EYRING, in "Handbook Physics and Chemistry of Rare Earths", Vol. 3, edited by K. A. Gschneider Jr and L. Eyring (North-Holland, Amsterdam, 1979) Ch. 27, p. 337.
5. P. KUNZMANN and L. EYRING, *J. Solid State Chem.* **14** (1975) 229.
6. L. EYRING, in "Non-Stoichiometric Oxides", edited by O. T. Sörensen (Academic Press, New York, 1981) Ch. 7, p. 337.
7. P. KNAPPE and L. EYRING, *J. Solid State Chem.* **58** (1985) 312.
8. C. BOULESTEIX and L. EYRING, *ibid.* **75** (1988) 291.
9. M. GASGNIER, G. SCHIFFMACHER, D. SVORONOS and P. CARO, *J. Microsc. Spectrosc. Electron.* **13** (1988) 13.
10. M. GASGNIER, G. SCHIFFMACHER and P. CARO, *Rev. de Phys. Appl. (Paris)* **23** (1988) 1341.
11. D. BÄUERLE, "Chemical Processing with Lasers", Springer Series in Materials Science, Vol. 1 (Springer, Berlin, Heidelberg, 1986).
12. *Idem*, (ed.), "Laser Processing and Diagnostics", Springer Series in Chemical Physics, Vol. 39 (Springer, Berlin, Heidelberg, 1984).
13. *Idem, Appl. Phys. B* **46** (1988) 261.
14. M. ALAM, T. DEBROY, R. ROY and E. BRAVAL, *Appl. Phys. Lett.* **53** (1988) 1687.
15. D. V. FEDOSEEV, V. L. BUCHOVATS, I. G. VERSHAVSKAYA, A. V. LAVRENT'EV and B. V. DERJAGUIN, *Carbon* **21** (1983) 237.
16. M. ALAM, T. DEBROY and R. ROY *J. Am. Ceram. Soc.* **73** (1990) 733.
17. E. E. KHAWAJA, M. A. KHAN, F. F. AL-ADEL and Z. HUSSAIN, *J. Appl. Phys.* **68** (1990) 1205.
18. M. GASGNIER, G. SCHIFFMACHER, L. ALBERT, P. E. CARO, H. DEXPERT, J. M. ESTEVA, C. BLANCARD and R. C. KARNATAK, *J. Less-Common Metals* **156** (1989) 59.
19. M. GASGNIER, G. SCHIFFMACHER, L. EYRING and P. CARO, *ibid.* **127** (1987) 167.
20. M. GASGNIER, G. SCHIFFMACHER, D. R. SVORONOS and P. E. CARO, *Inorg. Chim. Acta* **140** (1987) 79.
21. M. GASGNIER, Thesis, Orsay (1973).
22. M. GASGNIER, J. GHYS, G. SCHIFFMACHER, CH. HENRY LA BLANCHETAIS, R. CARO, C. BOULESTEIX,

CH. LAIER and B. PARDO, *J. Less-Common Metals* **34** (1974) 131.
23. O. T. SÖRENSEN, in "Non-Stoichiometric Oxides", edited by O. T. Sörensen (Academic Press, New York, 1981) Ch. 1, p. 1.
24. M. GASGNIER, G. SCHIFFMACHER and P. CARO, *J. Mater. Sci.* **24** (1989) 2801.
25. M. WAUTELET, *Phys. Status Solidi (b)* **103** (1981) 703.
26. P. STAMPFLI and K. H. BENEMANN, *Progr. Surf. Sci.* **35** (1991) 161.
27. P. BRUESCH and W. BUHRER, *Z. Phys. B Condensed Matter* **70** (1981) 1.

Received 20 November 1992
and accepted 21 September 1993